MagNet: An Open-Source Database for Data-Driven Magnetic Core Loss Modeling

Haoran Li[†], Diego Serrano[†], Thomas Guillod[‡], Evan Dogariu[†], Andrew Nadler[‡], Shukai Wang[†], Min Luo[§], Vineet Bansal[†], Yuxin Chen[†], Charles R. Sullivan[‡] and Minjie Chen[†]
[†]*Princeton University, Princeton NJ, United States*
[‡]*Dartmouth College, Hanover NH, United States*
[§]*Plexim GmbH, Zurich, Switzerland*
Email: {haoranli, ds9056, edogariu, sw0123, minjie}@princeton.edu

2022 IEEE Applied Power Electronics Conference and Exposition (APEC) | 978-1-6654-0688-8/22/$31.00 ©2022 IEEE | DOI: 10.1109/APEC43599.2022.9773372

***Abstract*—This paper introduces an open-source database – *MagNet* – for data-driven magnetic core loss modeling. MagNet aims to support data-driven magnetics research by hosting a large amount of experimentally measured excitation waveform data for many materials across a variety of operating conditions. This database in its current state contains over 150,000 excitation waveforms for six ferrite materials - TDK{N27, N49, N87}, Ferroxcube{3C90, 3C94}, Fair-Rite{78} - in the 50 kHz to 500 kHz, 10 mT to 300 mT range for sinusoidal, triangle, and trapezoidal waveforms. This paper presents the purposes of building MagNet, introduces the data acquisition system and data format, discusses the data quality, and presents a few examples of using this database with data driven methods.**

***Index Terms*—power magnetics, core loss, machine learning, data-driven method, neural network**

I. Introduction

Magnetic components are critical in almost all power electronics systems. Typically with the largest component volume and significant power loss, magnetics have a great impact on the system performance and optimization. While there have been major strides in the modeling and analysis of power semiconductor devices and circuit topologies, the necessary advances in the modeling and design of power magnetic components and materials are lagging [1]–[5]. Core loss models are usually developed and tested on different datasets with unknown or unreported data quality [6]–[9]. An open-source core loss database with controlled data quality is needed and is the main focus of this research.

The core loss modeling of a magnetic component is a challenging task due to the complicated core loss mechanisms, the numerous factors involved (i.e., temperature, dc-bias, memory effects), and the fact that no fully satisfactory first-principle model is known. A widely used method to model the core loss is the Steinmetz Equation (SE) [10], [11], which is an empirical equation based on curve-fitting, employed to calculate the core loss per unit volume in magnetic materials subjected to sinusoidal magnetic flux. However, sinusoidal magnetic flux is only encountered in a small subset of power converter topologies. Magnetic components in power electronics systems often have magnetizing currents with significant harmonic components, e.g., triangular or trapezoidal waveforms. Many advanced methods have been developed for core loss modeling with non-sinusoidal waveforms. Some of these, including the improved generalized Steinmetz equation (iGSE), improved-improved generalized Steinmetz Equation (i^{2}GSE) [12]–[14], are listed in Table I. All of these models have known accuracy limitations for specific waveform types.

TABLE I
Number of Parameters used by Core Loss Models

Method	Core Loss (P_v)	#Param.
SE	$k f^{\alpha} \hat{B}^{\beta}$	3
iGSE	$\frac{1}{T}\int_0^T k_i \lvert\frac{dB}{dt}\rvert^{\alpha}(\Delta B)^{\beta-\alpha}dt$	3
i^{2}GSE	$\frac{1}{T}\int_0^T k_i \lvert\frac{dB}{dt}\rvert^{\alpha}(\Delta B)^{\beta-\alpha}dt + \Sigma_{l=1}^{n} Q_{rl} P_{rl}$	8
ML	Neural Network	$\gg$10

Recent advances in data-driven methods, especially neural networks and other machine learning techniques, have proved extremely effective in solving non-linear multi-variable classification and regression problems, such as computer vision and speech recognition [15]–[17]. They have been applied to power electronics design and optimization [19]–[24]. An open-source, regularly maintained, high-quality database is the foundation of data-driven research. Just as ImageNet advances computer vision research [18], the goal of developing MagNet is to advance research in data-driven magnetic core loss modeling by providing a common ground for testing and comparing different magnetic materials, modeling methods, and design optimization tools. MagNet in its current state contains over 150,000 excitation waveforms for six ferrite materials - TDK{N27, N49, N87}, Ferroxcube{3C90, 3C94}, Fair-Rite{78} - in the 50 kHz to 500 kHz, 10 mT to 300 mT range for sinusoidal, triangle, and trapezoidal waveforms.

This paper is organized as follows: Section II introduces the data acquisition system of MagNet, including the hardware setup and software configurations; Section III discusses the considerations on data quality evaluation and methods to improve the data quality. Section IV introduces the database structure and data format in their current states. Section V presents a few example applications of MagNet including curve-fitting of Steinmetz parameters, core loss prediction based on equations, scalar-to-scalar core loss prediction,

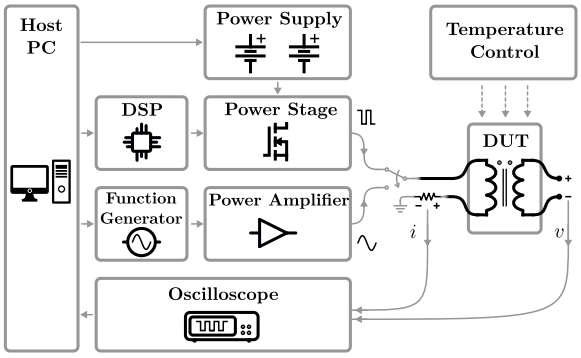

Fig. 1. Overview of the magnetic core loss data acquisition system of MagNet.

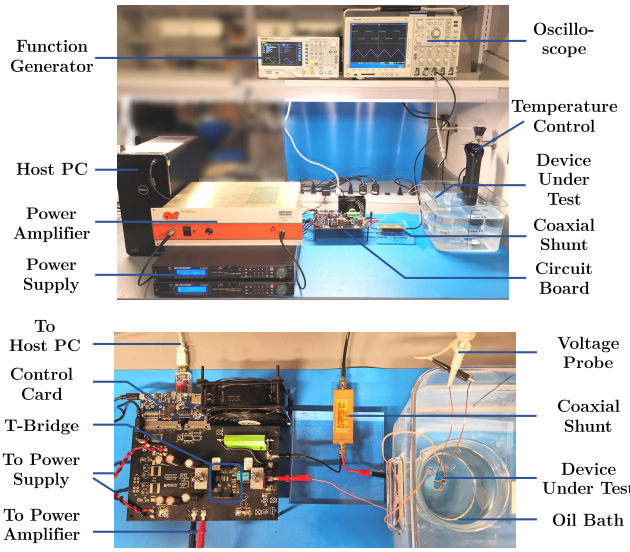

Fig. 2. Experiment setup and circuit configuration of the magnetic core loss data acquisition system of MagNet.

sequence-to-scalar core loss prediction, and transfer learning methods for modeling the core loss. Finally, Section VI concludes this paper.

II. Data Acquisition for MagNet

Magnetic core loss can be impacted by many factors including frequency, peak flux density, dc bias current, waveform shape, temperature, and many others. To capture the impact of all these factors, a fully automated data acquisition with carefully evaluated accuracy is needed. Figure 1 depicts an overview of the data acquisition system that is supporting MagNet, comprising a power stage which is capable of generating excitation waveforms, the Device Under Test (DUT), voltage measurement, current measurement, and temperature control. Figure 2 illustrates the experimental setup. This data acquisition system can automatically excite and drive the magnetic device under test with programmed excitations and measure the material responses. With this system, the magnetic core loss is directly measured and calculated via voltamperometric method, which has high simplicity and flexibility of operation [8], [25]–[27].

In this particular design, the power electronics circuit is capable of synthesizing triangle and trapezoidal flux waveforms with PWM driving signals through a micro-controller (Texas Instruments F38279D controlCARD). GaN devices (GS66508B) are used as the power devices for fast switching. Additional, non-PWM waveforms (e.g., sinusoidal waveforms) are synthesized using a function generator (Rigol DG4102) and a power amplifier (Amplifier Research 25A250AMB). The DUT consists of a toroidal magnetic core, a primary winding, and a secondary winding. The primary winding is used for exciting the core. A wide-band coaxial shunt (T&M W-5-10-1STUD) measures the current in the primary winding for inferring the magnetic field strength (H), whereas the secondary winding is open-circuited and used for inferring the magnetic flux density (B) by measuring the voltage across its terminals. The signal measurement and data acquisition are conducted using an oscilloscope (Tektronix DPO4054). In addition, this experimental setup includes a blocking capacitor connected in series with the DUT to eliminate the dc bias current. A large water tank, an oil bath, and a water heater (Anova AN400) are also included in the system to enable measurement at a particular temperature and to reduce undesired temperature variation during the measurement.

Python-based software on the host PC is designed and programmed to control and coordinate with the hardware system to enable fully automated equipment setting and core loss measurement. The software has three major functions: (a) communication with the power stage (power supplies, micro-controller and function generator) to transmit the waveform properties for each test, including the frequency, voltage and waveform shape, so that the power stage can synthesize and generate the desired excitations; (b) communication with the oscilloscope to set the configuration of signal sampling and data acquisition, and receive the measured digitized waveforms; (c) storing the collected data points and formatting them into the expected dataset structure. These three functions are executed in sequence within a multi-level iteration loop that sweeps the entire parameter space automatically. With this hardware-software combined system, each magnetic core loss data point only takes 1.2 second to measure. The system can, fully autonomously, collect around 3,000 data points per hour.

III. Data Quality Evaluation

The accuracy of a data-driven method is limited by the quality of the data. Measuring the magnetic core loss accurately across a wide operation range is challenging. The error distribution may be impacted by many factors. The measurement error may come from: parasitics in the circuit boards and wires, distortion and inaccuracy caused by the oscilloscope channels and probes, timing skew between channels, jitter in the micro-controller, electrical noise and quantization noise, temperature variation, etc.

The experimental setup and calibration process were designed following the recommendations in [25]–[27]. The calibration and measurement processes are fully automated. Human influence is minimized during the calibration and data acquisition process. We evaluated the systematic error

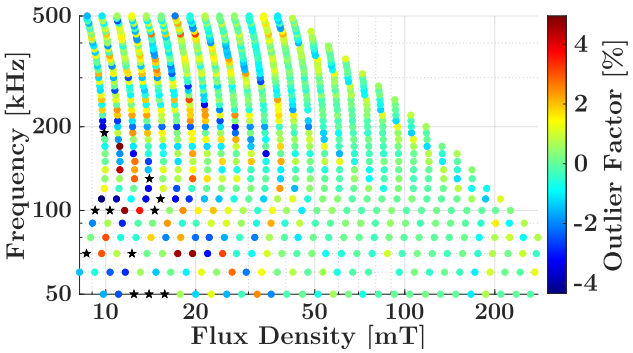

Fig. 3. Example of outlier datapoints in a dataset for the material N87 under sinusoidal excitation. For each point, data up to 0.1 decades far in terms of flux density and frequency are used to generate the local Steinmetz parameters. The datapoints discarded because the error compared to the estimation is above 5% are marked as black stars.

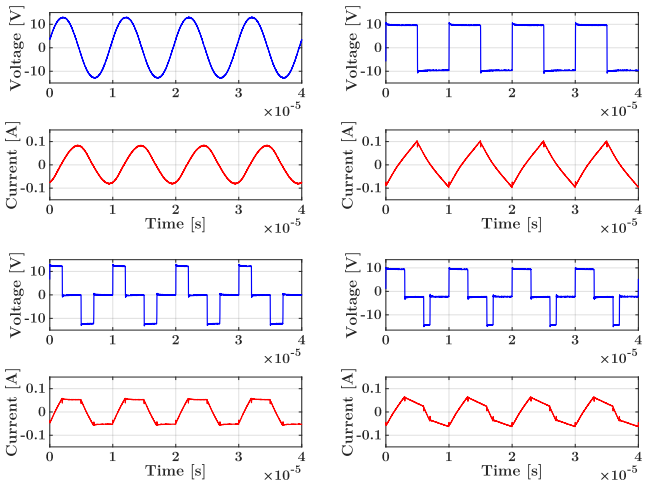

Fig. 4. Example voltage and current waveforms of sinusoidal, triangle, symmetric trapezoidal, and asymmetric trapezoidal excitations.

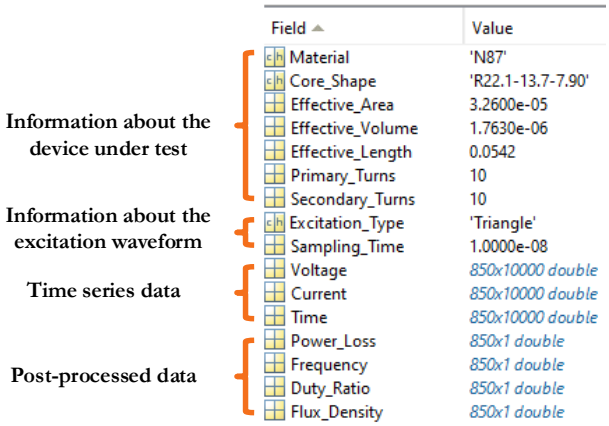

Fig. 5. Data format of the MagNet with four different data domains. The data are available in different formats: “MAT” , “JSON”, “HDF5”, and “CSV”. This data structure is designed to contain sufficient information for the research community to verify and reproduce the core loss measurement, and to trace the potential error mechanisms in the data acquisition process.

and statistical error of the data acquisition system by model-driven and data-driven methods and estimated the relative error for each material across the full operation range under test. High measurement accuracy is achieved in the main operation range, while the measurements for magnetic materials with high quality factor at high-frequency and low-amplitude ranges could be more prone to error.

Moreover, an algorithm was developed to detect and delete the outlier data points caused by rare anomaly operations based on smoothness analysis. For each point in the dataset, the estimated power losses are calculated based on the Steinmetz parameters inferred from the points that are close in terms of frequency and flux density to the considered point. If the measured losses of the data point are far from this estimated value, the data point can be considered an outlier. Figure 3 shows an example of the discrepancies between the expected losses based on the Steinmetz parameters of nearby points and the measured losses for different data points. A data point with high outlier factor is considered as a low-quality measurement and is removed from the dataset.

This outlier detection algorithm is just one example way of evaluating the data quality and removing noisy data. It has its own strengths and limitations, and it cannot detect systematic error. A systematic discussion of data quality, measurement accuracy evaluation, and techniques to improve the data quality is beyond the scope of this paper.

IV. Database Structure and Data Format

A large amount of magnetic core loss data is measured and collected by the data acquisition system. Figure 4 shows the voltage and current waveforms of four example measured data, including sinusoidal, triangle, symmetric trapezoidal, and asymmetric trapezoidal. The sampling time step is set as 10 ns, and each waveform sequence contains 10,000 sampling points.

Figure 5 shows the data format of MagNet in its current state, comprising four data domains: 1) information about the DUT, including material and geometry; 2) information about the excitation waveforms, including excitation type and sampling time step; 3) measured time-series data, including voltage, current, and time stamp; and 4) post-processed data, including power loss, frequency, duty ratio, and peak flux density. The data are available in different formats: “MAT” , “JSON”, “HDF5”, and “CSV”. This data structure is designed to contain sufficient information for the research community to verify and reproduce the core loss measurement, and to trace the potential error mechanisms in the automatic data acquisition process.

Table II lists the size of the MagNet dataset in its current state. The sizes of the data for the six unique materials are different because of their various designated operation ranges and step sizes for the parameter sweeping. All the measurements currently are conducted at zero dc-bias current condition and 25°C. Measurements with non-zero dc-bias current and different temperatures are in preparation.

An open-source web-based platform with graphical user in-

TABLE II
NUMBER OF DATA POINTS CURRENTLY IN THE MAGNET DATASET

Material	Sine	Tri.	Trap.	Total
TDK N27	1037	9106	16147	26290
TDK N49	1144	8991	16318	26453
TDK N87	965	9023	15750	25738
Ferroxcube 3C90	946	8758	15330	25034
Ferroxcube 3C94	1079	9072	16315	26466
Fair-Rite 78	980	9051	15850	25881
Total	6151	54001	95710	155862

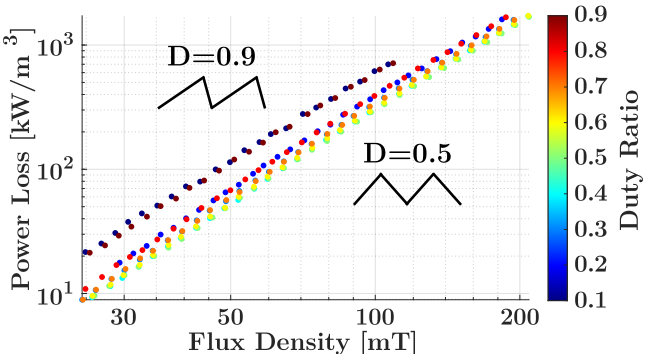

(a)

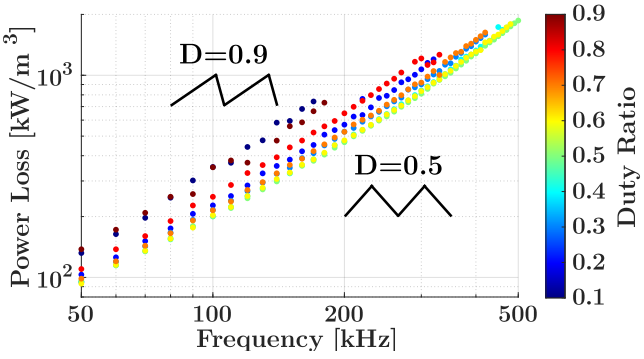

(b)

Fig. 6. Visualization of the measured core loss data under triangle excitation for N87 material: (a) core loss versus peak flux density with frequency at 200 kHz; (b) core loss versus frequency with peak flux density around 120 mT.

terface (GUI) - Mag-Net[1] - has been developed and is currently hosted by Princeton University. It is powered by Streamlit, and shared in GitHub, offering a variety of data-visualization tools for graphical user interface with the database. The website allows the dataset to be visualized in many ways, and enables rapid comparison of the core loss data of different materials. Figure 6 shows an example way to visualize the core loss in different duty cycles. The website provides access to the raw data being collected from the equipment before any post-processing with the test conditions documented. Core loss modeling algorithms including iGSE and other methods are also deployed on the website for online core loss estimation.

A circuit simulation tool (e.g. PLECS) is employed behind the user interface of the Mag-Net web page, which provides

[1]Princeton Mag-Net Website: https://mag-net.princeton.edu/

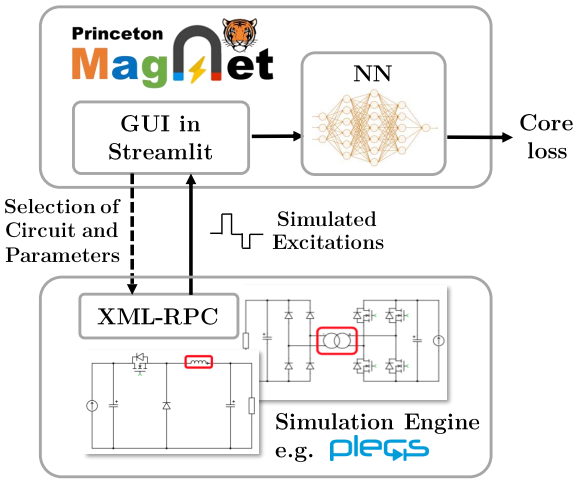

Fig. 7. Circuit simulation engine deployed behind the Mag-Net website for magnetic-in-circuit simulation.

inputs for the machine learning algorithm in combination with power converter operations, as shown in Fig. 7. Users can choose from a pool of common topologies (e.g., Buck, Boost, Flyback, Dual-Active-Bridge), specify the circuit parameters and operating conditions, then the simulation engine outputs the excitation waveform of the magnetic component. The Mag-Net server collects the waveform and predicts the core loss using the algorithms available on the web server including iGSE and neural networks.

V. APPLICATIONS OF MAGNET DATABASE

The MagNet database can be used in many different ways. For power magnetics with sinusoidal, triangle, trapezoidal excitations, one can simply plot the data and read the core loss under a particular operating condition, and use the values in the design process. MagNet can also be used to develop equation-based analytical models for magnetic core loss, such as being used for identifying the Steinmetz parameters, or data-driven magnetic core loss models such as neural network models. In this paper, we demonstrate using MagNet to find the Steinmetz parameters for the iGSE model, then explore several neural network examples for core loss modeling.

A. Steinmetz Parameters and iGSE Core Loss Model

The improved generalized Steinmetz equation (iGSE) uses the Steinmetz parameters to model magnetic core loss under arbitrary excitation waveforms. The Steinmetz parameters can be found in a few different ways, including 1) directly using the manufacturer-provided parameters; 2) curve-fitting from measured data with sinusoidal excitation across the entire dataset; and 3) curve-fitting from measured data with triangle or trapezoidal excitation across the entire dataset. One can also find Steinmetz parameters with a portion of the dataset to focus on a smaller operation range (local curve-fitting). Different methods lead to different Steinmetz parameters. Based on the MagNet database, the iGSE core loss modeling results

TABLE III
iGSE TRIANGLE-WAVE MODELING RESULTS FOR N87, N49, AND N27 MATERIALS

Material	α	β	k_i	Avg. Err.	Max. Err.
N87	1.43	2.49	5.77E-12	14.56%	61.07%
N49	1.27	3.17	1.18E-12	15.09%	63.22%
N27	1.09	2.44	4.88E-10	14.44%	60.36%

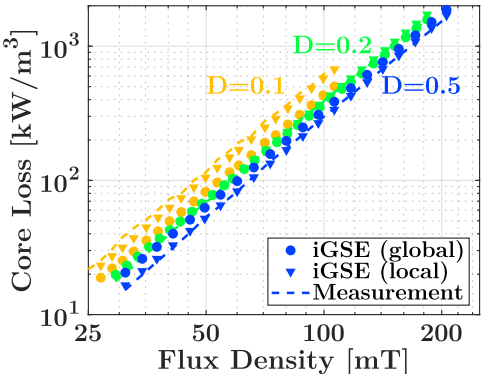

Fig. 8. iGSE predicted and measured results for N87 material under triangle excitation at 200 kHz. The parameters for iGSE (global) are obtained from the entire sinusoidal waveform dataset for N87, the parameters for iGSE (local) are obtained from the triangle waveform dataset for N87 within frequency range of 200±20 kHz.

for N87, N49, N27 materials under triangle excitation with Steinmetz parameters identified by method 2) above are listed in Table III, where the units are $\mathrm{kW/m^3}$ for losses, Hz for frequency and mT for flux density. To quantitatively evaluate the core loss prediction accuracy, the relative error between the measured core loss and the predicted core loss is defined as $|P_{measured} - P_{predicted}|/P_{measured}$. The average relative errors for the iGSE for triangle waves are consistently around 15% for the three materials.

Figure 8 shows an example comparison of the measured and iGSE-predicted core loss at an example operating point (200 kHz at 25°C). As the nature of curve-fitting across the entire dataset, the global iGSE performs well at some operating points, and perform poorly at other operating points. This is because the Steinmetz parameters usually vary over the range of operating points, especially frequency. Local curve-fitting helps to improve the prediction results at certain operation points. However, it requires multiple sets of Steinmetz parameters to cover the entire operation range. A neural network model naturally contains a large number of parameters to cover a wide operation range, and has the potential to outperform the iGSE method for predicting the core loss under a variety of operating conditions.

B. Feed-forward Neural Network Core Loss Model

Feed-forward neural networks (FNNs) are some of the simplest and most widely used artificial neural networks, and have proved to be effective tools for solving multi-variable nonlinear regression problems. We used an FNN as an example to develop a core loss model for ferrite materials under triangle excitations. Figure 9 illustrates the structure of a 5-layer FNN. This particular network has one input layer, one output layer, and three hidden layers. The input layer has three post-processed parameters as the input variables: the frequency f, the peak flux density B, and the duty ratio D. The output layer has one parameter: the magnetic core loss density of the material P_V. Each of the three hidden layers has multiple neurons. The precise number of neurons used in each layer is to be optimized. This model has a similar input/output configuration as the Steinmetz equation but has much more parameters available to capture a wide operating range.

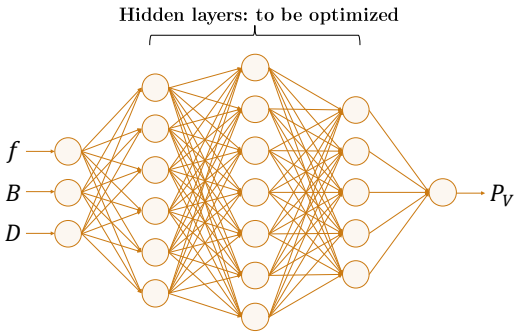

Fig. 9. Structure of an example 5-layer feed-forward neural network with three inputs (f, B, D) and one output (P_V). The structures and number of neurons in the hidden layers can be optimized. There is a trade-off between model size and model accuracy.

The network model is synthesized and trained with PyTorch [28]. The activation function is selected as ReLU to provide the capability of learning non-linearity, and the loss function for the network training is selected as mean-squared-error (MSE) of the logarithm value of core loss to ensure uniform performance across the entire operating range. The training optimizer is set as Adam [29]. An exponentially decayed learning rate strategy is implemented to get a better model convergence, where the initial learning rate is 0.02 and the decaying rate is 50% per 200 epochs. To start with, the dataset of N87 material in the MagNet database is selected, and the dataset is randomly split into two parts as 80% and 20%. The first part is further split into five subsets to conduct a K-fold ($K = 5$) training and cross-validation of the candidate networks, while the second part is kept aside untouched as the test set.

To determine the number of neurons in each hidden layer, we need to consider the trade-off between the network size and network performance. A small network may have limited learning capability and cannot provide good predictions, while a large network is more prone to overfitting. To analyze the relationship between the network size and prediction performance, we firstly set multiple boundaries for the number of neurons in each layer. An optimization tool – Optuna [30] – is selected to automatically search for the optimal number of neurons in each layer within each range. Table IV lists the search range for the number of neurons in each layer, the local optimal number of neurons, and the average and maximum relative error of the prediction results on the test set for five

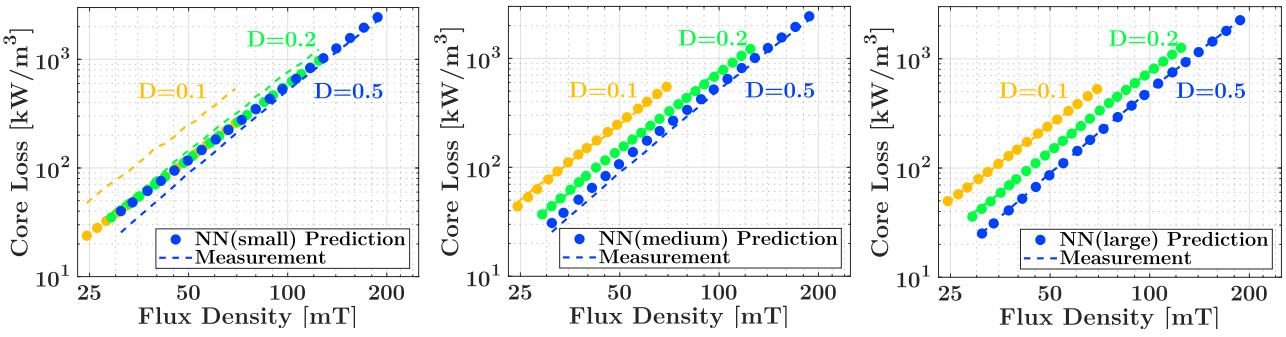

Fig. 10. Prediction results of three neural network core loss models for the N87 material at 300 kHz: (a) small scale; (b) medium scale; (c) large scale.

TABLE IV
PERFORMANCE OF A FEW DIFFERENT FNN MODELS WITH DIFFERENT SIZES FOR N87 MATERIAL WITH TRIANGLE-WAVE EXCITATION

Network Search Range	Neurons in Hidden Layers	Total Number of Parameters	Avg. Relative Error on Test Set	Max. Relative Error on Test Set
$[1, 4]$	2,1,3	21	19.76%	68.59%
$[4, 8]$	5,8,4	109	9.81%	47.72%
$[8, 16]$	15,15,9	454	5.33%	21.36%
$[16, 32]$	29,27,23	1594	1.81%	9.47%
$[32, 64]$	44,57,47	5515	1.77%	8.62%

TABLE V
FNN MODELING RESULTS FOR N87,N27, AND N49 MATERIALS: AVERAGE RELATIVE ERROR ON THE TEST SET

Model	# Params.	N87	N27	N49
iGSE	3	14.56%	14.44%	15.09%
NN(2,1,3)	21	19.76%	19.24%	25.45%
NN(5,8,4)	109	9.81%	6.76%	15.52%
NN(44,57,47)	5515	1.77%	1.63%	4.38%

FNNs with different scales. The total number of parameters in each neural network is also listed. As expected, the larger the neural network, the better the prediction performance.

After the automatic search process in Optuna, three neural networks with different numbers of hidden layers neurons are selected for case study, including NN(2,1,3), NN(5,8,4), and NN(44,57,47), noted as the small-scale network, the medium-scale network, and the large-scale network, respectively. The three numbers indicate the number of neurons in the three layers. Fig. 10 compares the prediction results of the three different neural network models for N87 material under triangle excitation with different duty ratios, and Table V shows a comparison of the modeling results for the three materials contained in the database. The results demonstrate that the performance of a small neural network can achieve is comparable to that of the iGSE for triangular waveforms. As the size of the neural network increases, the accuracy of core loss prediction improves. The large neural network can achieve an average relative error on the test set of below 5%.

C. More Efficient Machine Learning with Transfer Learning

Sometimes, it is unrealistic for designers to build a core loss measurement platform and collect sufficient high-quality data for model training, especially if there are multiple types of impact factors in the design process. As has been presented in [31], the MagNet enables us to explore transfer learning techniques to overcome the data limitations. Transfer learning is a technique in machine learning (ML) that focuses on storing knowledge gained while solving one problem and applying it to a different but related problem.

A major hypothesis behind applying transfer learning to magnetic core loss modeling is that similar physical mechanisms govern the core loss of similar magnetic materials under similar excitations. As a result, leveraging the large amount of core loss data in MagNet, we can firstly build a pre-trained generic model that captures the common patterns and characteristics of magnetic core loss, and further use it to support the development of the core loss models for other new materials, new excitations, new temperature, or new dc-bias through transfer learning.

We take material-to-material transfer learning as an example to explain the key concepts. The main motivation of transfer learning is to reduce the required size of the dataset from the new material. Three experiments are designed as illustrated in Fig. 11 to validate the hypothesis and examine the effectiveness of the transfer learning method: (a) select four materials from the MagNet database (N27, N49, 3C90, 3C94) and use their large amount of core loss data (i.e., a few thousands of data points) to train a pre-trained model (same structure as the (15,15,9) FNN mentioned in Sec. V-B); (b) select another material from the MagNet database (N87), which is treated as the target material that has limited amount of core loss data available, and re-train the pre-trained model with only a small amount of data; (c) for comparison, directly train a randomly initialized neural network with the same small amount of data.

Fig. 12 shows the decreasing of the testing average relative error as the increasing of the amount of data used for retraining for the reference model and the pre-trained model, for an example training process with N87 material under triangular excitation. The pre-trained model only needs 50 new data points to achieve steady-state average relative error of 5%, while it takes about $3,000$ new data points for a randomly

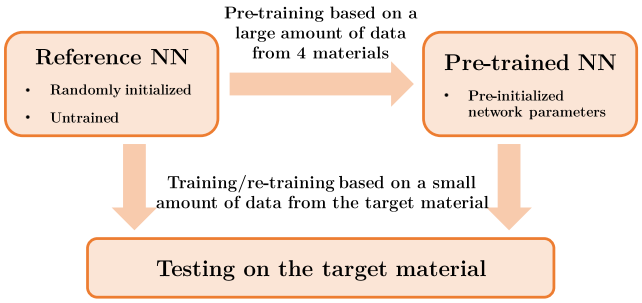

Fig. 11. Key principle of transfer learning for magnetic core loss modeling.

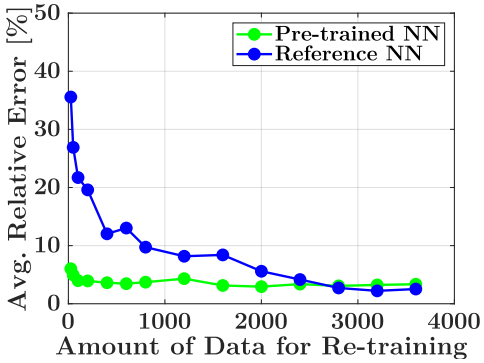

Fig. 12. Testing average relative error rates after training the reference FNN and re-training the pre-trained FNN with a varied amount of data.

initialized reference model to achieve similar average relative error. The amount of data needed for retraining the neural network for a new material is significantly reduced.

D. Long Short-Term Memory Network Core Loss Model

We develop a sequence-to-scalar model with time sequence of excitation voltage $v(t)$ (or the flux density $B(t)$, more generally) as the input and volumetric power loss as the output. The long short-term memory (LSTM) network is one of the most commonly used neural networks for regression problems with sequential input [32], [33]. LSTM networks are well-suited to classifying, processing, and making predictions based on time series data, especially if there are sophisticated correlations (e.g., memory effects) among time series. An example structure of the LSTM-based magnetic core loss model is demonstrated in Fig. 13. The input layer of the LSTM takes the entire voltage waveform as a sequence input. The output of LSTM is aggregated and loaded with a FNN to perform core loss regression. In this example design, the LSTM has 32 units and the FNN comprises three hidden layers. The output of the FNN is the volumetric magnetic core loss for this particular sequence of excitation.

To validate the effectiveness of this LSTM-based core loss model, the network shown in Fig. 13 is synthesized and trained with PyTorch. A merged dataset that contains all three types of waveforms (sinusoidal, triangle, and trapezoidal) is now selected. They are randomly split into training set, validation set, and test set for the LSTM model.

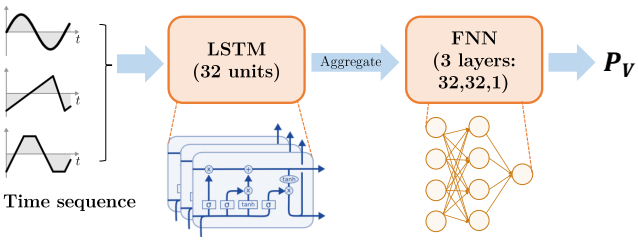

Fig. 13. Structure of an example LSTM neural network followed by a FNN to predict the magnetic core loss based on time sequence input.

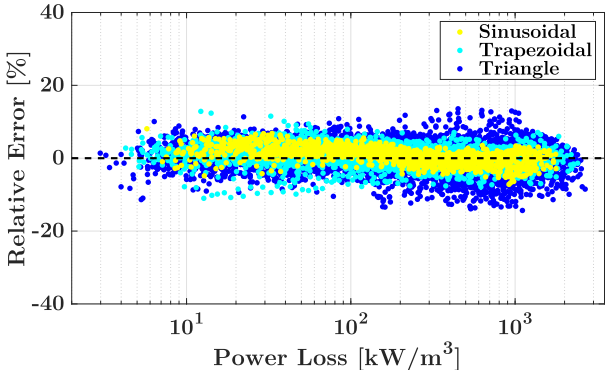

Fig. 14. Testing relative error distribution of the LSTM-based core loss model.

TABLE VI
LSTM MODELING RESULTS FOR N87 MATERIAL

Type of Waveform	Average of Relative Errors	RMS of Relative Errors	Maximum of Relative Errors
Sinusoidal	1.86%	2.33%	8.08%
Triangle	2.41%	3.19%	14.35%
Trapezoidal	1.95%	2.58%	12.85%
Overall	2.09%	2.78%	14.35%

Figure 14 shows the error distribution between the measured core loss and the predicted core loss achieved by the LSTM-based model. More prediction results are listed in Table VI. As observed, the proposed LSTM model achieves a good core loss prediction accuracy for all three types of waveforms, where the relative error approximately has an even and unbiased distribution close to 0%. The overall average of relative error (absolute value) is around 2% and the maximum relative error is within 15%. The LSTM model contains $5,569$ parameters in total, which is closed to the large-scale FNN mentioned in Sec. V-B. This LSTM-based model is able to make core loss prediction for all three types of waveforms. The applicability of this LTSM model is not restricted by the scalar representation of waveform shapes. It can be used to predict core loss for excitation waveforms which are not included in the database. This ability to generalize to arbitrary waveforms is an important objective, as with the iGSE and similar methods, but the accuracy of this model when used this way has yet to be tested.

VI. Conclusions

This paper presents an open-source large-scale database – *MagNet* – for data-driven magnetic core loss modeling. This database in its current state contains over $150,000$ excitation waveforms for six ferrite materials under sinusoidal, triangle, and trapezoidal excitation waveforms. An open-source data visualization framework and website make the data easily accessible for multiple purposes.

Several example applications of the MagNet database have been explored. With the magnetic core loss data, one can extract the Steinmetz parameters for a particular material within certain operation range, and calculate the core loss based on analytical models such as the iGSE. The database can be used to develop more advanced analytical core loss models. The database can also be used to train neural networks (e.g., scalar-to-scalar, sequence-to-scalar, sequence-to-sequence, or transfer learning models), and can predict the core loss in different operating conditions. The neural networks can provide comparable or even more accurate core loss predictions than traditional empirical models. We anticipate that with the constantly increasing scale, data quality, and waveform diversity, MagNet can offer unique opportunities to researchers in power electronics, power magnetics, and data science.

Acknowledgements

This work was jointly supported by the DOE ARPA-E DIFFERENTIATE program and the Schmidt DataX Fund at Princeton University made possible through a major gift from the Schmidt Futures Foundation.

References

[1] D. J. Perreault et al., "Opportunities and Challenges in Very High Frequency Power Conversion," *Twenty-Fourth Annual IEEE Applied Power Electronics Conference and Exposition*, 2009, pp. 1-14.

[2] C. R. Sullivan, B. A. Reese, A. L. F. Stein and P. A. Kyaw, "On Size and Magnetics: Why Small Efficient Power Inductors Are Rare," *International Symposium on 3D Power Electronics Integration and Manufacturing (3D-PEIM)*, 2016, pp. 1-23.

[3] Y. Han, G. Cheung, A. Li, C. R. Sullivan and D. J. Perreault, "Evaluation of Magnetic Materials for Very High Frequency Power Applications," *IEEE Transactions on Power Electronics*, vol. 27, no. 1, pp. 425-435, Jan. 2012.

[4] A. J. Hanson, J. A. Belk, S. Lim, C. R. Sullivan and D. J. Perreault, "Measurements and Performance Factor Comparisons of Magnetic Materials at High Frequency," *IEEE Transactions on Power Electronics*, vol. 31, no. 11, pp. 7909-7925, Nov. 2016.

[5] M. Chen, M. Araghchini, K. K. Afridi, J. H. Lang, C. R. Sullivan and D. J. Perreault, "A Systematic Approach to Modeling Impedances and Current Distribution in Planar Magnetics," *IEEE Transactions on Power Electronics*, vol. 31, no. 1, pp. 560-580, Jan. 2016.

[6] W. Roshen, "Ferrite Core Loss for Power Magnetic Components Design," *IEEE Trans. on Magnetics.*, vol. 27, no. 6, pp. 4407-4415, Nov. 1991.

[7] D. Lin, P. Zhou, W. N. Fu, Z. Badics and Z. J. Cendes, "A Dynamic Core Loss Model for Soft Ferromagnetic and Power Ferrite Materials in Transient Finite Element Analysis," *IEEE Trans. on Magnetics.*, vol. 40, no. 2, pp. 1318-1321, March 2004.

[8] M. Mu, Q. Li, D. J. Gilham, F. C. Lee, and K. D. T. Ngo, "New Core Loss Measurement Method for High-Frequency Magnetic Materials," *IEEE Trans. on Power Electron.*, vol. 29, no. 8, pp. 4374–4381, Aug. 2014.

[9] M. Luo, D. Dujic and J. Allmeling, "Modeling Frequency Independent Hysteresis Effects of Ferrite Core Materials using Permeance–Capacitance Analogy for System-Level Circuit Simulations," *IEEE Trans. on Power Electron.*, vol. 33, no. 12, Dec. 2018.

[10] C. P. Steinmetz, "On the Law of Hysteresis," *Proceedings of the IEEE*, vol. 9, no. 2, pp. 3-64, 1892.

[11] J. B. Goodenough, "Summary of Losses in Magnetic Materials," *IEEE Trans. Magn.*, vol. 38, no. 5, pp. 3398–3408, Sep. 2002.

[12] J. Li, T. Abdallah and C. R. Sullivan, "Improved Calculation of Core Loss with Nonsinusoidal Waveforms," *IEEE Industry Applications Conference Annual Meeting*, Chicago, IL, USA, 2001, pp. 2203-2210, vol.4.

[13] J. Mühlethaler, J. Biela, J. W. Kolar and A. Ecklebe, "Improved Core-Loss Calculation for Magnetic Components Employed in Power Electronic Systems," *IEEE Trans. on Power Electron.*, vol. 27, no. 2, pp. 964-973, Feb. 2012.

[14] E. Stenglein, T. Düerbaum, "Core Loss Model for Arbitrary Excitations with Dc Bias Covering a Wide Frequency Range," in *IEEE Transactions on Magnetics*, vol. 57, no. 6, pp. 1-10, 2021.

[15] Y. LeCun, Y. Bengio and G. Hinton, "Deep Learning," *Nature*, vol. 521, pp. 436–444, May 2015.

[16] J. Schmidhuber, "Deep Learning in Neural Networks: An Overview," in *Neural Networks*, vol. 61, pp. 85-117, 2015.

[17] B. Widrow and M. A. Lehr, "30 years of Adaptive Neural Networks: Perceptron, Madaline, and Backpropagation," in *Proceedings of the IEEE*, vol. 78, no. 9, pp. 1415-1442, 1990.

[18] J. Deng, W. Dong, R. Socher, L. Li, K. Li and Li Fei-Fei, "ImageNet: A Large-Scale Hierarchical Image Database," *IEEE Conference on Computer Vision and Pattern Recognition*, 2009, pp. 248-255.

[19] S. Zhao, F. Blaabjerg and H. Wang, "An Overview of Artificial Intelligence Applications for Power Electronics," *IEEE Transactions on Power Electronics*, vol. 36, no. 4, pp. 4633-4658, April 2021.

[20] T. Guillod, P. Papamanolis and J. W. Kolar, "Artificial Neural Network (ANN) based Fast and Accurate Inductor Modeling and Design," *IEEE Open Journal of Power Electronics*, vol. 1, pp. 284-299, 2020.

[21] H. Li, S. R. Lee, M. Luo, C. R. Sullivan, Y. Chen and M. Chen, "MagNet: A Machine Learning Framework for Magnetic Core Loss Modeling," *IEEE 21st Workshop on Control and Modeling for Power Electronics (COMPEL)*, 2020, pp. 1-8.

[22] E. I. Amoiralis, P. S. Georgilakis, T. D. Kefalas, M. A. Tsili and A. G. Kladas, "Artificial Intelligence Combined with Hybrid FEM-BE Techniques for Global Transformer Optimization," *IEEE Transactions on Magnetics*, vol. 43, no. 4, pp. 1633-1636, April 2007.

[23] C. Nussbaum, H. Pfutzner, T. Booth, N. Baumgartinger, A. Ilo and M. Clabian, "Neural Networks for the Prediction of Magnetic Transformer Core Characteristics," *IEEE Transactions on Magnetics*, vol. 36, no. 1, pp. 313-329, Jan. 2000.

[24] G. K. Miti, and A. J. Moses, "Neural Network-based Software Tool for Predicting Magnetic Performance of Strip-Wound Magnetic Cores at Medium to High Frequency," *IEEE Proceedings - Science, Measurement and Technology*, vol. 151, no. 3, pp. 181-187, 2 May 2004.

[25] E. Stenglein, D. Küebrich, M. Albach, T. Düerbaum, "Guideline for Hysteresis Curve Measurements with Arbitrary Excitation: Pitfalls to Avoid and Practices to Follow," *International Exhibition and Conference for Power Electronics, Intelligent Motion, Renewable Energy and Energy Management (PCIM Europe)*, Nuremberg, Germany, 2018.

[26] E. Stenglein, B. Kohlhepp, D. Kübrich, M. Albach and T. Dürbaum, "GaN-Half-Bridge for Core Loss Measurements Under Rectangular AC Voltage and DC Bias of the Magnetic Flux Density," in *IEEE Transactions on Instrumentation and Measurement*, vol. 69, no. 9, pp. 6312-6321, 2020.

[27] M. Luo, D. Dujic and J. Allmeling, "Test Setup for Characterisation of Biased Magnetic Hysteresis Loops in Power Electronic Applications," *2018 International Power Electronics Conference (IPEC-Niigata 2018 - ECCE Asia)*,pp. 422-427, Niigata, Japan, 2018.

[28] A. Paszke, S. Gross and F. Massa, *et al.*"PyTorch: an Imperative Style, High-Performance Deep Learning Library," *33rd Conference on Neural Information Processing Systems (NeurIPS 2019)*, Vancouver, Canada, 3 Dec. 2019.

[29] D. P. Kingma, J. Ba, "Adam: A Method for Stochastic Optimization," *International Conference on Learning Representations (ICLR)*, 2015.

[30] T. Akiba, S. Sano, T. Yanase, T. Ohta, and M. Koyama, "Optuna: a Next-Generation Hyperparameter Optimization Framework," *Proceedings of the 25rd ACM SIGKDD International Conference on Knowledge Discovery and Data Mining*, 2019.

[31] E. Dogariu, H. Li, S. Wang, M. Luo and M. Chen, "Transfer Learning Methods for Data-Driven Magnetic Core Loss Modeling," *IEEE Workshop on Control and Modeling of Power Electronics (COMPEL)*, 2021.

[32] X. Li and X. Wu, "Constructing Long Short-Term Memory based Deep Recurrent Neural Networks for Large Vocabulary Speech Recognition," *IEEE International Conference on Acoustics, Speech and Signal Processing (ICASSP)*, South Brisbane, QLD, Australia, 2015.

[33] F. A. Gers, N. N. Schraudolph and J. Schmidhuber, "Learning Precise Timing with LSTM Recurrent Networks," *Journal of Machine Learning Research*, vol. 3, pp. 115-143, 2002.